ELSEVIER

Journal of Fluorine Chemistry 110 (2001) 109–116

JOURNAL OF FLUORINE CHEMISTRY

www.elsevier.com/locate/jfluchem

Transition metal sulfur dioxide hexafluoroarsenates and hexafluoroantimonates

E. Lork[a], R. Mews[a,*], J. Petersen[a], M. Schröter[a], B. Žemva[b]

[a]*Institute of Inorganic and Physical Chemistry, University of Bremen, P.O. Box 330440, D-28334 Bremen, Germany*
[b]*Department of Inorganic Chemistry and Technology, "Jožef Stefan" Institute, Jamova 39, 1000 Ljubljana, Slovenia*

Received 7 November 2000; accepted 3 December 2000

Abstract

The preparation and characterization by X-ray crystallography of transition metal sulfur dioxide hexafluoroarsenates of the general formula $[M(SO_2)_x](AsF_6)_2$ **1** (**1a**: M = Mn, $x = 2$; **1c**: M = Co, $x = 4$; **1e**: M = Cu, $x = 4$) and the hexafluoroantimonate $[Co(SO_2)_2](SbF_6)_2$ **3** is reported. The structural features of the compounds mentioned are compared with those of $[Fe(SO_2)_4](AsF_6)_2$ (**1b**) and $[Ni(SO_2)_6](AsF_6)_2$ (**1d**), reported previously. The structural diversity of transition metal sulfur dioxide complexes is discussed. © 2001 Elsevier Science B.V. All rights reserved.

Keywords: Sulfur dioxide complexes; Transition metal hexafluoroarsenates; Hexafluoroantimonates; X-ray structures

1. Introduction

Although a number of reports on the coordination chemistry of sulfur dioxide transition metal hexafluoroarsenates $[M(SO_2)_x](AsF_6)_2$ (**1**) is found in the literature [1], most of the starting materials used in these reactions are poorly characterized. Due to the weakly coordinated SO_2 ligands and the almost not interacting AsF_6^- counter ions, in SO_2 as a solvent the metal centers in these complexes are almost "naked". Even extremely weak donors, e.g. OPF_3 [2] can be introduced as ligands. Compounds of type **1** can be readily prepared by the oxidation of the appropriate metals with AsF_5 in liquid SO_2, as has been shown independently by Dean [3] and Desjardins and Passmore [4], Dean also extended this method to hexafluoroantimonates [3]. The unequivocal characterization of the SO_2 complexes is difficult because of their thermal instability. SO_2 is readily lost, the number x of the SO_2 ligands coordinated to the metal centers in these complexes is mostly not known with certainty. Simon and co-workers structurally characterized the first metal sulfur dioxide complexes containing only the SO_2 ligands besides weakly interacting anions. From the system $LiCl/AlCl_3/SO_2$ they isolated $\{[Li(\mu\text{-}OSO)_{6/2}]\ AlCl_4\}_n$ [5], where the Li-centers are homoleptically coordinated by six OO′-bridging SO_2 ligands, from the system $NaCl/AlCl_3/SO_2$, $\{Na[AlCl_4]\cdot 1.5SO_2\}_n$ was characterized. The sodium centers are octahedrally coordinated containing terminal O– and bridging OO′–SO_2 ligands as well as bridging $AlCl_4$-tetrahedra [6].

In *trans*-$[Mg(OSO)_2(\mu\text{-}F_2AsF_4)_{4/2}]_n$, each Mg atom is coordinated by two O-bonded SO_2 ligands in *trans*-positions to each other, the Mg centers are connected by *cis*-bridging AsF_6^- octahedra to infinite chains [7]. More recently, we reported the structures of *cis*-$[Fe(OSO)_4(FAsF_5)_2]$ (**1b**) and $[Ni(OSO)_6](AsF_6)_2$ (**1d**) [8,9], the latter complex is the only homoleptic transition metal sulfur dioxide complex known. In all of these structurally characterized complexes, the metal centers are differently coordinated, the structures vary with the metal centers and with the counter ions. In the present paper, we extend the structural investigations to the hexafluoroarsenates of Mn, Co and Cu(II) and to the Co sulfur dioxide hexafluoroantimonate.

2. Results and discussion

Similar to the procedures described previously [3,4,7] onto powders of the appropriate transition metals, SO_2 was condensed via a vacuum line followed by addition of a slight excess of AsF_5 according to the stoichiometry in Eq. (1)

$$M + 3AsF_5 \xrightarrow{SO_2} [M(SO_2)_x](AsF_6)_2 + AsF_3 \quad (1)$$

* Corresponding author. Tel.: +49-421-218-3354; fax: +49-421-218-4267.
E-mail address: mews@chemie.uni-bremen.de (R. Mews).

PII: S0022-1139(01)00417-1

where for **1a**: M = Mn, $x = 2$; **1b**: M = Fe, $x = 4$; **1c**: M = Co, $x = 4$; **1d**: M = Ni, $x = 6$; **1e**: M = Cu, $x = 4$.

After removal of the byproduct AsF_3 at −20 to −10°C under vacuum, the residue was redissolved in SO_2. In the presence of small amounts of additional AsF_5, the salts were crystallized by slow evaporation of the solvent (see Section 4). The numbers x given in Eq. (1) result from X-ray structure determinations. Because of the thermal lability of the complexes, they readily lose SO_2; therefore, elemental analyses always show a too small sulfur content. IR-spectra indicate the presence of SO_2 ligands ($\nu_{as}(SO_2) = 1330\ cm^{-1}$; $\nu_{sym}(SO_2) = 1150\ cm^{-1}$). These data agree quite well with those reported in the literature [7], but due to the ready loss of SO_2, no reliable statements on the structures of the compounds can be made on this basis. The X-ray structures of compounds **1b** (M = Fe) and **1d** (M = Ni) we reported some time ago in a short communication [8,9]. Only for Ni was a homoleptic complex observed in the solid state. In solution, this might be true also for the other metals of Eq. (1) but during the crystallization process, the counterion AsF_6^- partially displaces SO_2 ligands. Due to the higher Lewis acidity of SbF_5 in comparison to AsF_5 [10], we expected for SbF_6^- inferior donor properties; even with Co a homoleptic complex seemed likely [1]. The Co (sulfur dioxide)hexafluoroantimonate was prepared in two steps from CoF_2 and SbF_5 in anhydrous HF followed by dissolving the resulting product in liquid SO_2

$$CoF_2 + SbF_5 \xrightarrow{HF} \underset{\mathbf{2}}{Co(SbF_6)_2} \quad (2)$$

$$Co(SbF_6)_2 + SO_{2exe} \xrightarrow{SO_2} \underset{\mathbf{3}}{[Co(SO_2)_2](SbF_6)_2} \quad (3)$$

Excess of SbF_5 was removed in the first step at room temperature under vacuum, recrystallization of the remaining residue from SO_2 gave **3**, showing an even a smaller number of SO_2 ligands connected to the metal center than in **1c**.

3. Structure investigations on transition metal sulfur dioxide hexafluoroarsenates and hexafluoroantimonates

Details of the structure determinations for $[Mn(OSO)_2(\mu\text{-}F_2AsF_4)_{4/2}]_n$ (**1a**) $[Co(OSO)_4(FAsF_5)_2]$ (**1c**), $[Co(OSO)_2(\mu\text{-}F_2SbF_4)_2]_n$ (**3**) and $[Cu(OSO)_4(FAsF_5)_2]$ (**1e**) are given in Table 1. Fig. 1 shows the coordination sphere of a Mn center of **1a** with selected bond distances and angles. In Fig. 2 the connection of these centers by bridging (μ-F_2AsF_4) to a three-dimensional (3D) network is represented. In Figs. 3–7, the structures of **1c**, **1e** and **3** are given, those of $[Fe(OSO)_4(FAsF_5)_2]$ (**1b**) and $[Ni(OSO)_6](AsF_6)_2$ (**1d**) reported previously in a preliminary communication [8,9] are added for completeness. A common feature of all structures is the octahedral environment of the metal centers, but Figs. 1–7

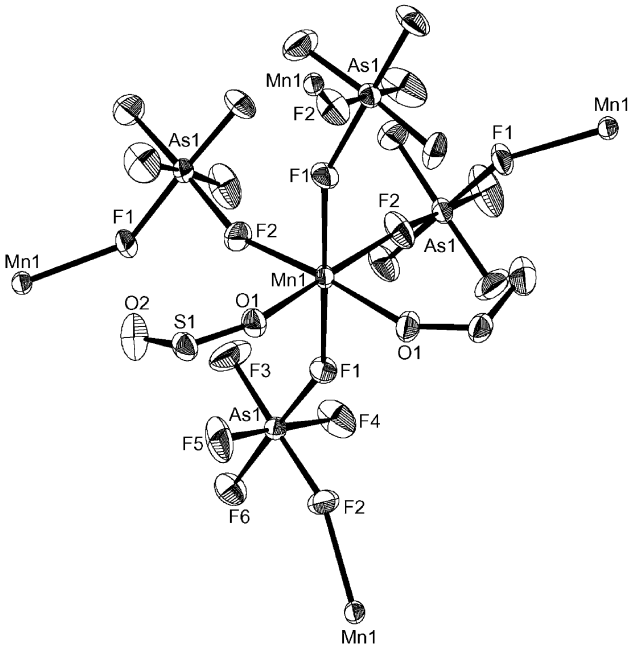

Fig. 1. Selected bond distances (pm) and bond angles (°) for $[Mn(OSO)_2(F_2AsF_4)_{4/2}]_n$ **1a**. Mn(1)–F(2) 211.1(3), Mn(1)–F(1) 214.5(2), Mn(1)–O(1) 215.1(3), O(1)–S(1) 144.1(3), S(1)–O(2) 139.9(4), F(1)–As(1) 176.8(3) As(1)–F(4) 167.6(4), As(1)–F(3) 168.7(4), As(1)–F(5) 168.8(3), As(1)–F(6) 169.7(3), As(1)–F(2) 176.1(3) F(2)–Mn(1)–F(2) 95.7(2), F(2)–Mn(1)–F(1) 87.77(11), F(2)–Mn(1)–F(1) 87.46(11), F(2)–Mn(1)–O(1) 88.00(13), F(1)–Mn(1)–O(1) 95.42(12), F(1)–Mn(1)–O(1) 89.68(12), O(1)–Mn(1)–O(1) 88.39(19), S(1)–O(1)–Mn(1) 148.8(2), O(2)–S(1)–O(1) 117.0(2), As(1)–F(1)–Mn(1) 148.33(14), As(1)–F(2)–Mn(1) 157.65(16).

demonstrate the structural diversity of these transition metal sulfur dioxide complexes. Differences not only result from varying the transition metal center but also from variation of the counter ion, even compounds with the same stoichiometry, the same number of SO_2 ligands coordinated (**1a** and **3**) exhibit different structures. In the manganese complex **1a**, the two SO_2 ligands are arranged in a *cis*-position. Each of the coordinated AsF_6^- counter ions connects to different Mn-centers, from the *cis*-bridging of these anions, a 3D network results. Both SO_2-ligands are equivalent (Mn−O = 215.1(3) pm), but two different Mn–F distances are observed. Those in *trans*-positions to the SO_2-ligands (Mn−F2 = 211.1(3) pm) are shorter than those where the hexafluoroarsenates are in a *trans*-position to each other (Mn−F1 = 214.5(2) pm).

In the mononuclear complex $[Fe(OSO)_4(FAsF_5)_2]$ **1b**, from the high spin electron configuration $t_{2g}^4e_g^2$ two nonequivalent positions in the octahedral coordination sphere result. If the fourth t_{2g} electron is placed in the equatorial *xy*-plane, it can be readily explained why the apical Fe–F2 (201.4(6) pm and Fe–O1 distances (207.5(7) pm) are significantly shorter than the distances to the equatorial ligands (Fe–F12 207.9(5), Fe–O3 212.3(6), Fe–O5 210.5(7), Fe–O7 211.5(6) pm).

Table 1
Crystal data and structure refinement for **1a**, **1c**, **1e**, and **3**[a]

	1a	**1c**	**1e**	**3**
Empirical formula	$As_2F_{12}MnO_4S_2$	$As_2CoF_{12}O_8S_4$	$As_2CuF_{12}O_8S_4$	$CoF_{12}O_4S_2Sb_2$
Formula weight	560.90	693.01	697.62	658.55
Temperature	173(2) K	173(2) K	173(2) K	173(2) K
Wavelength	71.073 pm	71.073 pm	71.073 pm	71.073 pm
Crystal system	Orthorhombic	Monoclinic	Monoclinic	Triclinic
Space group	Fdd2	$P2_1/c$	$P2_1/c$	$P\bar{1}$
Unit cell dimensions	$a = 1506.8(2)$ pm $b = 1791.6(3)$ pm $c = 921.2(2)$ pm $\alpha = 90^\circ$ $\beta = 90^\circ$ $\gamma = 90^\circ$	$a = 850.8(4)$ pm $b = 1355.6(8)$ pm $c = 1473.5(6)$ pm $\alpha = 90^\circ$ $\beta = 99.36(3)^\circ$ $\gamma = 90^\circ$	$a = 750.50(10)$ pm $b = 1296.9(2)$ pm $c = 890.7(2)$ pm $\alpha = 90^\circ$ $\beta = 104.210(10)^\circ$ $\gamma = 90^\circ$	$a = 502.60(10)$ pm $b = 774.87(10)$ pm $c = 855.53(10)$ pm $\alpha = 94.921(10)^\circ$ $\beta = 91.770(10)^\circ$ $\gamma = 97.860(10)^\circ$
Volume	2.4869(8) nm^3	1.6768(14) nm^3	0.8404(3) nm^3	0.32853(7) nm^3
Z	8	4	2	1
Density (calculated)	2.996 mg/m^3	2.745 mg/m^3	2.757 mg/m^3	3.329 mg/m^3
Absorption coefficient	6.843 mm^{-1}	5.595 mm^{-1}	5.860 mm^{-1}	5.802 mm^{-1}
F(0 0 0)	2104	1316	662	301
Crystal size	0.6 mm × 0.3 mm × 0.3 mm	0.5 mm × 0.4 mm × 0.4 mm	0.6 mm × 0.5 mm × 0.5 mm	0.70 mm × 0.30 mm × 0.20 mm
Range (θ) for data	2.83–27.50°	2.80–26.01°	2.80–27.50°	2.66–27.49°
Index ranges	$-19 \le h \le 19$, $-23 \le k \le 23$, $-1 \le l \le 11$	$-1 \le h \le 10$, $-1 \le k \le 16$, $-18 \le l \le 18$	$-1 \le h \le 9$, $-1 \le k \le 16$, $-11 \le l \le 11$	$-1 \le h \le 6$, $-10 \le k \le 10$, $-11 \le l \le 11$
Reflections collected	3339	4371	2604	2044
Independent reflections	922 (R(int) = 0.0535)	3284 (R(int) = 0.0597)	1924 (R(int) = 0.0411)	1506 (R(int) = 0.0146)
Absorption correction	None	DIFABS	Empirical	DIFABS
Refinement method	Full-matrix least-squares on F^2	Full-matrix least-squares on F^2	Full-matrix least-squares on F^2	Full-matrix least-squares on F^2
Data/restraints/parameters	922/1/97	3284/0/244	1924/0/125	1506/0/98
Goodness-of-fit on F^2	1.083	0.872	1.037	1.225
Final R indices [$I > 2\sigma(I)$]	$R_1 = 0.0221$, $wR_2 = 0.0555$	$R_1 = 0.0371$, $wR_2 = 0.0782$	$R_1 = 0.0409$, $wR_2 = 0.1039$	$R_1 = 0.0241$, $wR_2 = 0.0657$
R indices (all data)	$R_1 = 0.0233$, $wR_2 = 0.0562$	$R_1 = 0.0596$, $wR_2 = 0.0824$	$R_1 = 0.0517$, $wR_2 = 0.1103$	$R_1 = 0.0256$, $wR_2 = 0.0665$
Absolute structure parameter	0.005(14)	–	–	–
Extinction coefficient	0.00180(11)	–	0.0129 (16)	0.0045(10)
Largest diffraction peak and hole	0.731 and −0.398 e $Å^{-3}$	0.683 and −0.758 e $Å^{-3}$	0.931 and −1.008 e $Å^{-3}$	1.633 and −0.829 e $Å^{-3}$

[a] Details in common: ω–2θ scans; Siemens P4 diffractometer; refinement based on F^2; $R_1 = \Sigma||F_o| - |F_c||\Sigma||F_o|$; $wR_2 = \{\Sigma[w(F_o^2 - F_c^2)]/\Sigma[w(F_o^2)^2]\}^{1/2}$, Programs and SHELX-97 [13] and DIAMOND [14].

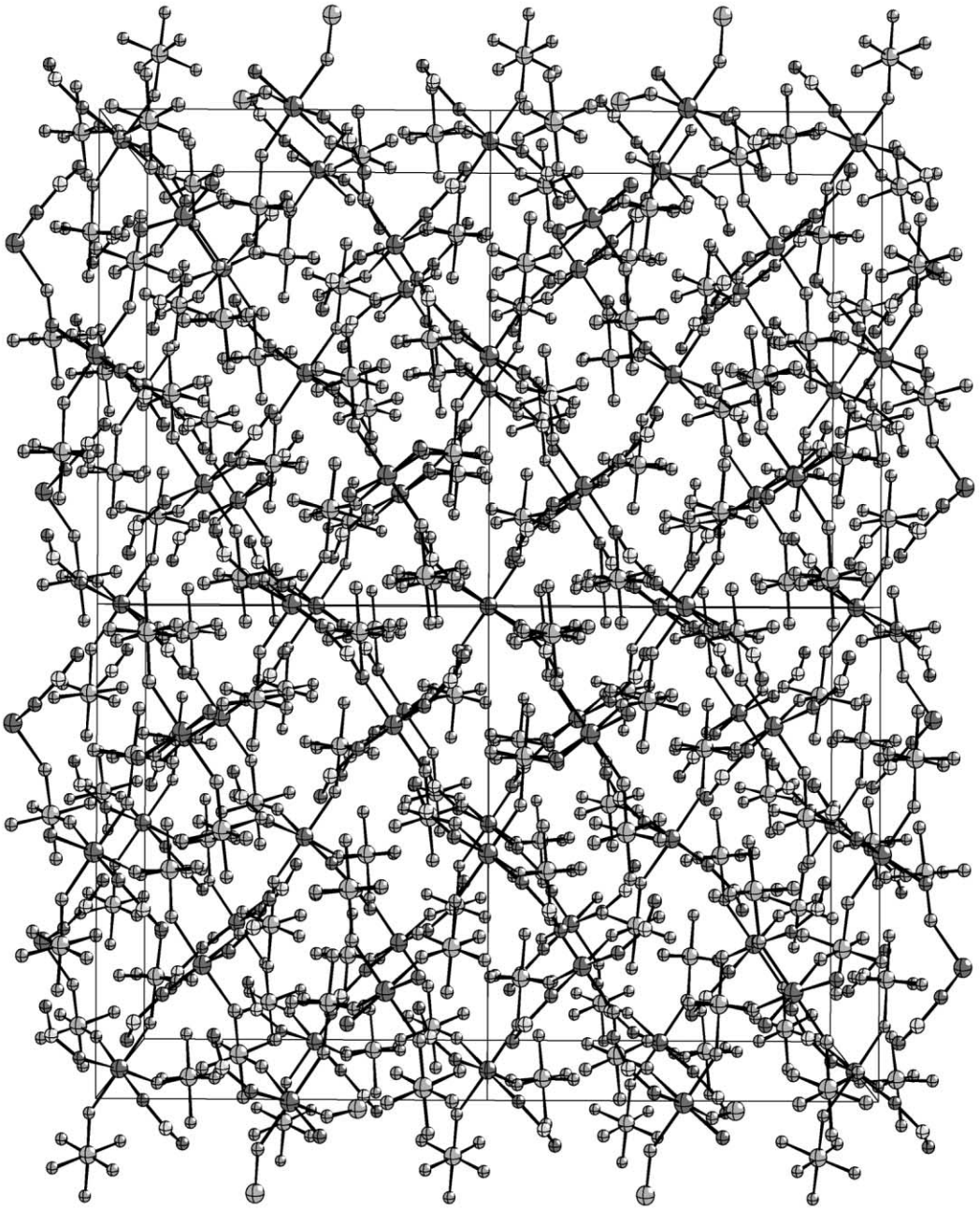

Fig. 2. Representation of the crystal packing of **1a**.

In *cis*-$[Co(OSO)_4(FAsF_5)_2]$ **1c**, no significant difference between the two Co–F (201.8(3) and 202.6(3) pm) and the four Co–O distances (205.9(4)–207.5(4) pm) are observed. In $[Ni(OSO)_6](AsF_6)_2$ **1d** the Ni–O-distances vary only from 203.3(3) to 204.4(3) pm.

The differences between *trans*-$[Cu(OSO)_4(FAsF_5)_2]$ **1e** and *cis*-$[Co(OSO)_4(FAsF_5)_2]$ **1c** are readily explained by the d^9-electron configuration of Cu(II) and the resulting Jahn–Teller distortion. Compared to **1a**–**d**, this leads to a longer apical metal fluorine (220.3(2) pm) and a shorter equatorial metal oxygen bond (197.1(3), 197.5(3) pm).

In *trans*-$[Co(OSO)_2(\mu\text{-}F_2SbF_4)_{4/2}]_n$, the Co-centers are connected by *cis*-bridging bidentate SbF_6^- anions to form infinite chains of eight membered $(CoFSbF–)_2$ heterocycles, a structural type previously observed for *cis*-$[Mg(OSO)_2(\mu\text{-}F_2AsF_4)_{4/2}]$ [7]. A more detailed comparison of these two heterocycles shows distinct differences in the conformation, as indicated in Fig. 8. In $(Mg–F–AsF–)_2$ an envelope-type conformation is found, while in **3** the centrosymmetric ring system adopts a chair conformation. All the atoms except As(1) are virtually in one plane. The Co–F distances in **3** are slightly longer than those in the corresponding

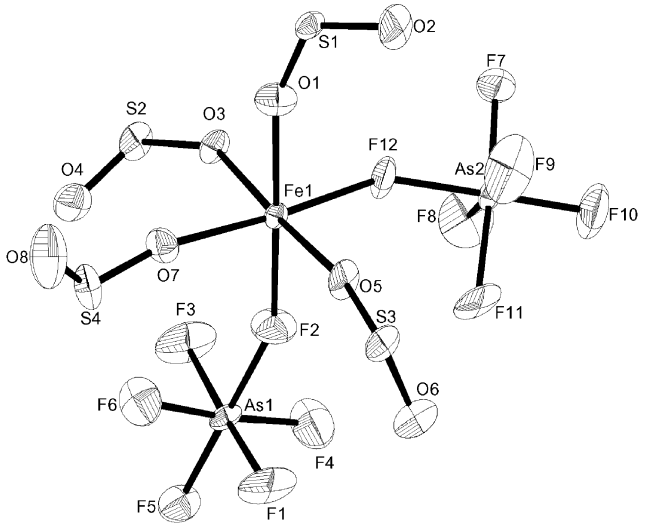

Fig. 3. Selected bond distances (pm) and bond angles (°) for $[Fe(OSO)_4(FAsF_5)_2]$ **1b**. Fe(1)–F(2) 201.4(6), Fe(1)–O(1) 207.5(7), Fe(1)–F(12) 207.9(5), Fe(1)–O(5) 210.5(7), Fe(1)–O(7) 211.5(6), Fe(1)–O(3) 212.3(6), S(1)–O(2) 139.9(8), S(1)–O(1) 143.5(7), S(2)–O(4) 141.8(7), S(2)–O(3) 144.4(7), S(3)–O(6) 139.7(9), S(3)–O(5) 141.7(7), S(4)–O(8) 137.3(9), S(4)–O(7) 141.4(7), As(1)–F(2) 180.2(6), As(2)–F(12) 176.2(5), O(2)–S(1)–O(1) 117.5(5), S(1)–O(1)–Fe(1) 157.7(5), O(4)–S(2)–O(3) 117.4(4), S(2)–O(3)–Fe(1) 142.6(4), O(6)–S(3)–O(5) 117.2(5), S(3)–O(5)–Fe(1) 164.5(5), O(8)–S(4)–O(7) 119.4(5), S(4)–O(7)–Fe(1) 164.1(5), As(2)–F(12)–Fe(1) 148.2(3).

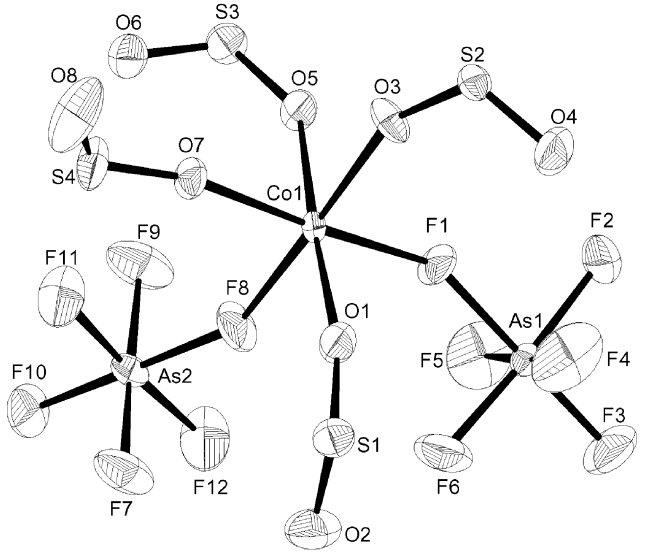

Fig. 4. Selected bond lengths (pm) and angles (°) for $[Co(OSO)_4(FAsF_5)_2]$ **1c**. Co(1)–F(8) 201.8(3), Co(1)–F(1) 202.6(3), Co(1)–O(3) 205.9(4), Co(1)–O(1) 207.2(4), Co(1)–O(5) 207.5(4), Co(1)–O(7) 207.5(4), As(1)–F(1) 177.5(3), As(2)–F(8) 178.4(3), S(1)–O(2) 139.5(5), S(1)–O(1) 141.1(4), S(2)–O(4) 140.1(4), S(2)–O(3) 143.0(4), S(3)–O(6) 140.1(4), S(3)–O(5) 144.2(4), S(4)–O(8) 137.6(6), S(4)–O(7) 141.5(4), As(2)–F(8)–Co(1) 154.6(2), O(2)–S(1)–O(1) 117.6(3), S(1)–O(1)–Co(1) 162.9(3), O(4)–S(2)–O(3) 118.0(3), S(2)–O(3)–Co(1) 154.4(3), O(6)–S(3)–O(5) 117.2(3), S(3)–O(5)–Co(1) 142.7(2), O(8)–S(4)–O(7) 119.8(3), S(4)–O(7)–Co(1) 163.8(3).

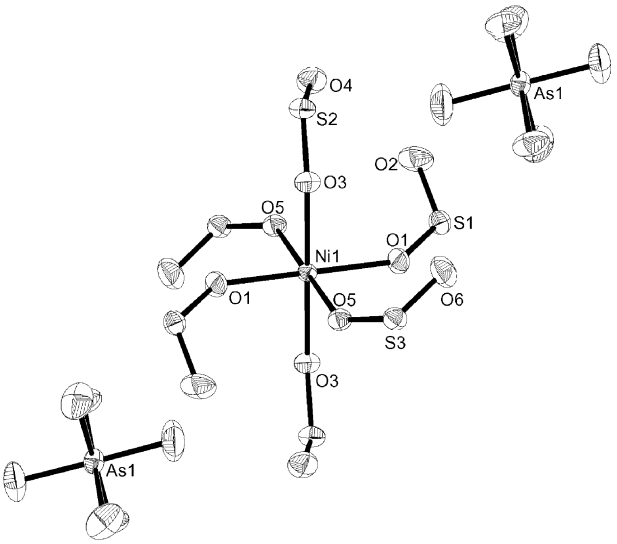

Fig. 5. Selected bond lengths (pm) and angles (°) for $[Ni(SO_2)_6](AsF_6)_2$ **1d**. Ni(1)–O(1) 204.4(3), Ni(1)–O(3) 203.5(3), Ni(1)–O(5) 203.3(3), S(1)–O(1) 144.3(4), S(1)–O(2) 141.8(4), S(2)–O(3) 145.0(4), S(2)–O(4) 141.5(4), S(3)–O(5) 144.9(4), S(3)–O(6) 140.5(4), O(1)–S(1)–O(2) 116.9(2), Ni(1)–O(1)–S(1) 145.6(2), O(3)–S(2)–O(4) 117.5(2), Ni(1)–O(3)–S(2) 145.0(2), O(5)–S(3)–O(6) 116.2(2), Ni(1)–O(5)–S(3) 139.8(2).

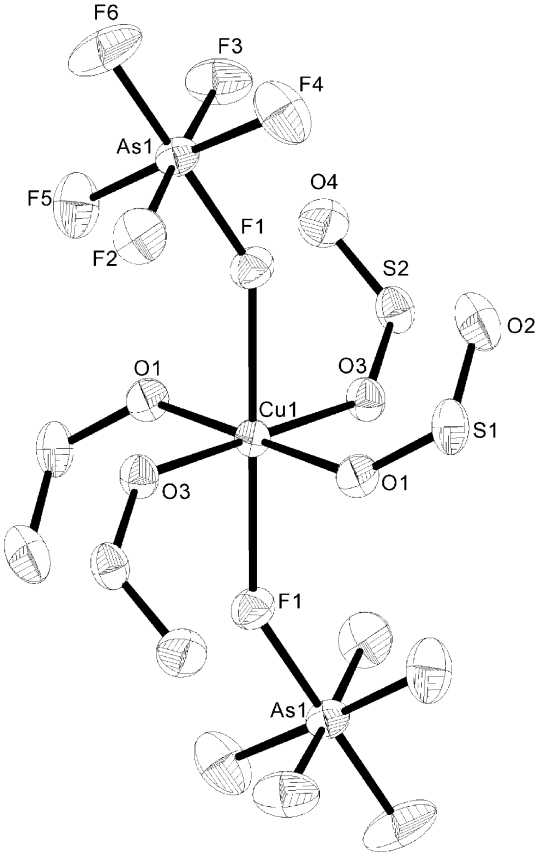

Fig. 6. Selected bond lengths (pm) and angles (°) for $[Cu(OSO)_4(FAsF_5)_2]$ **1e**. Cu(1)–O(1) 197.1(3), Cu(1)–O(3) 197.5(3), Cu(1)–F(1) 220.3(2), O(1)–S(1) 144.9(3), S(1)–O(2) 140.9(4), O(3)–S(2) 145.4(3), S(2)–O(4) 140.2(4), As(1)–F(1) 175.3(3), S(1)–O(1)–Cu(1) 137.4(2), O(2)–S(1)–O(1) 116.6(2), S(2)–O(3)–Cu(1) 139.0(2), O(4)–S(2)–O(3) 116.2(2).

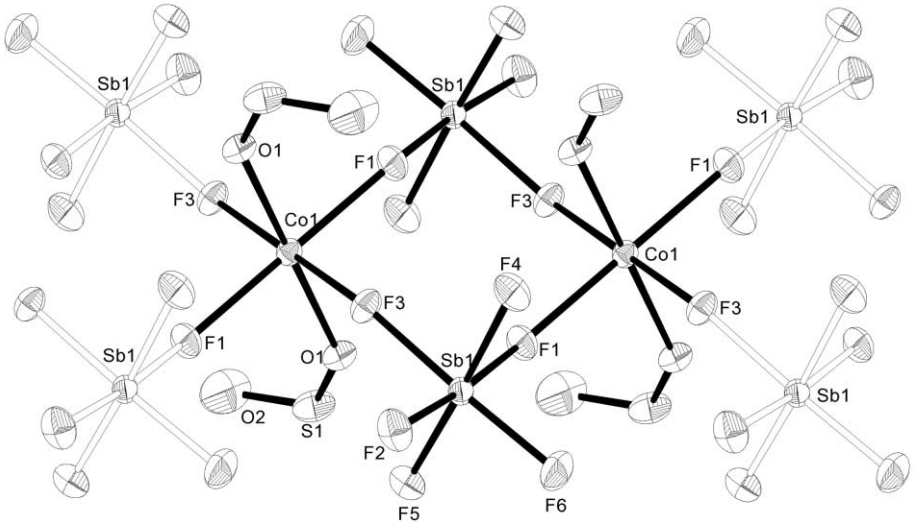

Fig. 7. Selected Bond lengths (pm) and angles (°) for $[Co[OSO)_2(\mu\text{-}F_2SbF_4)_{4/2}]_n$ **3**. Co(1)–O(1) 204.9(3), Co(1)–F(1) 206.0(2), Co(1)–F(3) 205.9(2), F(1)–Sb(1) 193.6(2), Sb(1)–F(6) 185.1(3), Sb(1)–F(4) 185.5(3), Sb(1)–F(2) 185.6(3), Sb(1)–F(5) 186.1(3), Sb(1)–F(3) 193.4(2), O(1)–S(1) 145.0(3), S(1)–O(2) 141.1(5) O(1)–Co(1)–O(1) 180.00(14), F(3)–Co(1)–F(1) (endocyclic) 90.24(10), F(3) –Co(1)–F(1) (exocyclic) 89.76(10), Sb(1)–F(1)–Co(1) 141.26(14), Co(1)–F(3)–Sb(1) 147.12(14), F(1)–Sb(1)–F(3) 84.90(11), F(2)–Sb(1)–F(6) 95.17(13).

hexafluoroarsenate **1c** and the Co–O-distances shorter, probably a result of the higher Lewis acidity of the Sb-centers. As expected the Sb–F distances to the bridging fluorine atoms are appreciably increased by the interaction with the Co-centers (to 193.5 pm) compared to 185.3 pm (average) found for the non-bridging Sb–F distances. In **3**, the Co-center is almost ideally octahedrally coordinated, the angles between adjacent atoms vary only between 88.7 and 91.3°. At the Sb-center, the endocyclic FSbF angle is reduced to 84.9°, while the exocyclic FSbF angle *trans* to F(1)Sb(1)F(3) is widened to 95.2°.

In Table 2, the averaged MF, MO and SO-distances of **1a–e** are listed. Subtraction of the appropriate ionic radii [11] from the corresponding MO and MF distances results in "radii" for oxygen in the SO_2 and for fluorine in AsF_6^- ligands. For the SO_2 ligand, a radius of 118–118.5 pm is found, that in the homoleptic $[Ni(OSO)_6]^{2+}$ cation is 2 pm longer. For Cu(II), which shows neither hexa- nor tetra-coordination, the observed MO distances correspond to an averaged coordination (see Table 2). A radius of 118–120 pm for the SO_2 ligand seems to be independent of the oxidation state and the coordination number of the metal centers. For $[Gd(OSO)_3(F_2AsF_4)_{6/2}]_n$ ($CN(Gd^{3+}) = 9$; $r = 124.7$ pm [10]) for which the data were also collected at −100°C, 118.3–120.3 pm were determined [12]. For $[Mg(OSO)_2(F_2AsF_4)_{4/2}]_n$ (a room temperature structure [7]), the unusually large SO_2 radii of 121.7 and 127.7 pm cast some doubt on the distances determined.

The slightly decreasing $r_{AsF_6^-}$ from **1a** to **1c** can be explained by an increase in the Lewis acidity of the metal centers with decreasing ionic radius. The different situation for the Cu(II) complex is reflected by the much larger $r_{AsF_6^-}$. $r_{AsF_6^-}$ is even more dependent on the charge of the metal centers. For the Gd complex described previously [12] for $r_{AsF_6^-}$ 108.3–109.3 pm is calculated.

For the noncoordinating AsF_6^- in **1d**, an average bond distance $d_{AsF} = 170.9$ pm is observed. Interaction with the metal centers stretches this bond to 176.2–180.2 pm, the smallest stretching is observed for the Cu complex **1d** (175.3 pm). Parallel to this elongation, a minor shortening of the other bonds up to 2 pm is found.

It seems that the data can be used as a check for the reliability of published structures and for predicting unknown structures.

Table 2
Averaged MF, MO, SO-distances of **1a–e** and "r_{SO_2}" and "r_{AsF_6}"

	r_{ion} (pm)	MF	MO	S–O_{br}	S–O_t	OSO	r_{SO_2}	r_{AsF_6}
Mn (**1a**)	97	212.8	215.1	144.1	139.9	117.0	118.1	115.8
Fe (**1b**)	92	204.6	210.4	142.8	139.7	117.9	118.4	114.3
Co (**1c**)	88.5	202.2	207.0	142.5	139.3	118.2	118.5	113.7
Ni (**1d**)	83	–	203.7	144.7	141.3	116.9	120.7	–
Cu (**1e**)	87 (CN6), 71 (CN4)	220.3	197.3	145.2	140.6	116.4	110.3, 126.3	141.3

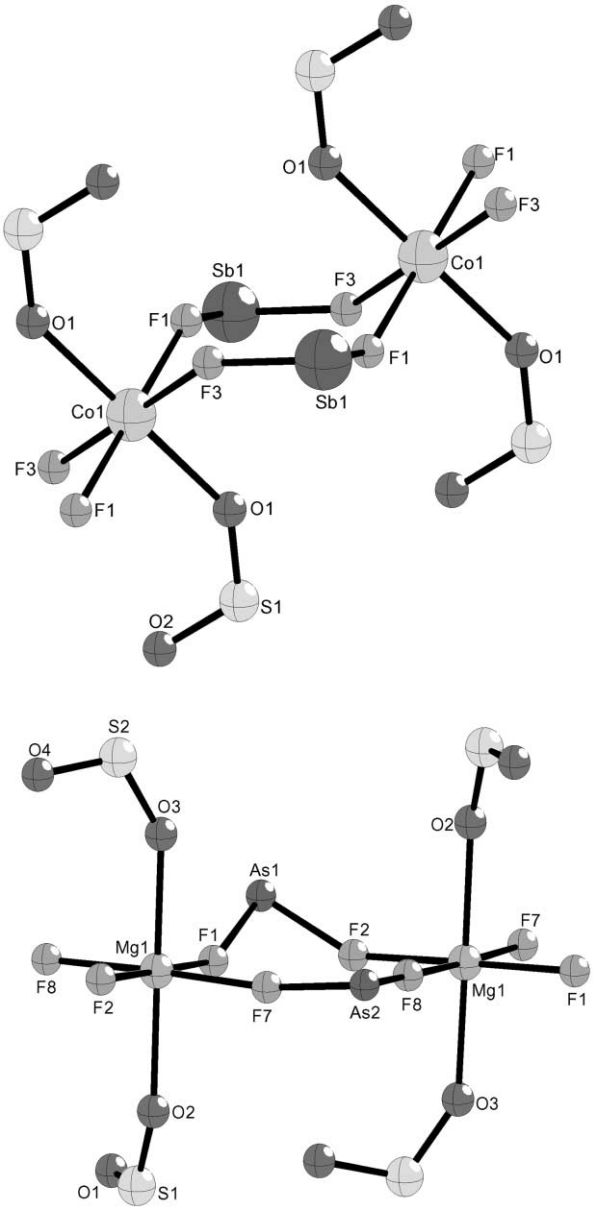

Fig. 8. Conformations of the eight membered metallaheterocycles (Co–F–Sb–F–)$_2$ in **3** and (Mg–F–As–F–)$_2$ in $[Mg(OSO)_2(\mu\text{-}F_2AsF_4)_{4/2}]_n$ [7].

4. Experimental

Compounds **1a–e** were prepared similarly to the procedures reported in the literature [3,4,7] by oxidation of the metal powders with a slight excess of AsF_5 in liquid SO_2 at room temperature using pressure-proof Schlenk-vessels with built-in sintered glass frits [11]. After filtration, the solvent was evaporated, the by-product, AsF_3, removed under vacuum at −20 to −10°C. For recrystallization, the resulting solids were dissolved in SO_2 containing some additional AsF_5, λ-shaped glass vessels with Teflon stop cocks were used. Single crystals were obtained by slow condensation of the solvent to the empty leg, kept at 0°C, from that containing the product solution at 0–5°C. Single crystals for the X-ray structure determinations were taken directly from SO_2-solutions cooled to −10°C.[1]

The IR-spectra of the solids corresponded quite well with those reported in the literature [7].

$Co[SbF_6]_2$ **2** and $[Co(OSO)_2(\mu\text{-}F_2SbF_4)_{4/2}]_n$ **3**: 5 ml of anhydrous HF and excess of SbF_5 were condensed onto 2.20 g (20.7 mmol) of CoF_2 in a PFA reaction vessel equipped with a stirring bar and a Teflon valve via a vacuum line. The reaction mixture was stirred for 1 h at room temperature. After removal of all volatiles overnight at room temperature under vacuum, 10.90 g **2** (20.55 mmol) remained as a pink powder, melting point above 350°C. – IR(Nujol mull): 738 cm^{-1} vs, 708 cm^{-1} vs, 671 cm^{-1} s, 584 cm^{-1} vs, 570 cm^{-1} sh, 516 cm^{-1}, 477 cm^{-1} sh.

3: 2.00 g (3.77 mmol) of **2** were stirred for 15 min in 10 ml of liquid SO_2 in a glass vessel equipped with a stirring bar and a Teflon valve until a clear solution resulted. After removal of all volatiles **3** remained as pink powder in quantitative yield (2.48 g). Single crystals were obtained similarly to compounds **1** by recrystallization at temperatures slightly below room temperature. –IR(Nujol-mull): 1333 cm^{-1} vs (ν_{sym} (SO_2)), 1199 cm^{-1} w, 1144 cm^{-1} vs (ν_{sym} (SO_2)), 730 cm^{-1} sh, 711 cm^{-1} vs, 672 cm^{-1} m, 649 cm^{-1} w, 600 cm^{-1} vs, 537 cm^{-1} sh, 522 cm^{-1} m.

Acknowledgements

One of us (B.Ž.) would like to thank the Alexander von Humboldt Foundation for the von Humboldt Research Award. Support by WTZ (Wissenschaftlich-technologische Zusammenarbeit Deutschland–Slowenien) (Project SLO-005-97) is also gratefully acknowledged.

References

[1] R. Mews, E. Lork, P.G. Watson, B. Görtler, Coord. Chem. Rev. 197 (2000) 277–320 (review paper).
[2] R. Mews, J. Chem. Soc., Chem. Commun. (1979) 278–279.
[3] P.A.W. Dean, J. Fluorine Chem. 5 (1975) 499–507.
[4] C.D. Desjardins, J. Passmore, J. Fluorine Chem. 6 (1975) 379–388.
[5] A. Simon, U. Peters, E.-M. Peters, H. Kühnl, B. Koslowski, Z. Anorg. Allg. Chem. 469 (1980) 94–100.
[6] K. Peters, A. Simon, E.-M. Peters, H. Kühnl, B. Koslowski, Z. Anorg. Allg. Chem. 492 (1982) 7–14.
[7] R. Hoppenheit, W. Isenberg, R. Mews, Z. Naturforsch 37b (1982) 1116–1121.
[8] E. Lork, J. Petersen, R. Mews, Angew. Chem. 106 (1994) 1724–1725.
[9] E. Lork, J. Petersen, R. Mews, Angew. Chem. Int. Ed. Engl. 33 (1994) 1663–1665.

[1] Crystallographic data for the structures in this paper have been deposited with the Fachinformationzentrum Karlsruhe (FIZ) as supplementary publication numbers CSD 411789, CSD 411790, CSD 411791 and CSD 411792. Copies of the data can be obtained, free of charge, on application to FIZ, abt. PROKA, 76344 Eggenstein-Leopoldshafen, Germany, (Tel.: +49-7247-808-205 or e-mail: crysdata@fiz-karlsruhe.de).

[10] K.O. Christe, D.A. Dixon, D. McLemore, W.W. Wilson, J. A Sheehy, J.A. Boatz, J. Fluorine Chem. 101 (2000) 151–153.
[11] R.D. Shannon, Crystal Radii in Oxides and Fluorides, in: B. King (Ed.), Encyclopedia of Inorganic Chemistry, Vol. 2, Wiley, Chichester, 1994, p. 929.
[12] J. Petersen, E. Lork, R. Mews, J. Chem. Soc., Chem. Commun. (1996) 2593–2594.
[13] G.M. Sheldrick, SHELX-97, University of Göttingen, Germany, 1997.
[14] Visual Structure Information System, DIAMOND CRYSTAL IMPACT, P.O. BOX 1251, D-53002 Bonn, Germany.